Delineation of groundwater potential zones of the transboundary aquifers within the semiarid Bulal catchment, Southern Ethiopia

Assaminew Gebeyehu (melijal1@gmail.com)
Addis Ababa University
Tenalem Ayenew
Addis Ababa University
Asfawossen Asrat
Botswana International University of Science and Technology

Research Article

Keywords: Groundwater potential zones (GWPZ), Borena, Bulal catchment, GIS-overlay analysis, Analytical hierarchical process (AHP), Transboundary aquifers, Semiarid

Posted Date: September 27th, 2022

DOI: https://doi.org/10.21203/rs.3.rs-2075414/v1

Abstract

Groundwater is the only reliable drought-resilient water source in the semiarid Bulal transboundary catchment located close to the Kenyan border. The central and southern parts of the catchment are dominantly overlain by Bulal basalts, while the Borena basement complex outcrops in the eastern part. This work aims to identify and delineate the groundwater potential zones of the semiarid Bulal catchment within the boundary of Ethiopia using integrated GIS and RS techniques in combination with the analytical hierarchal process (AHP). Ten input parameters were selected based on their relative significance to groundwater occurrence and movement. The normalized weights were assigned to the input themes and their individual features as per Saaty's AHP approach. A composite groundwater potential zone index (GWPZI) map was finally generated by integrating all the input layers employing the GIS-overlay analysis technique. The map was validated using the yield of wells from the catchment. The GWPZI map depicts four groundwater potential zones in the catchment: high (representing 27% of the total area), moderate (20%), low (28%) and very low (25%). The geological feature has the greatest influence on the distribution of groundwater potential in the catchment. Areas with high potential are mainly overlain by Bulal basaltic flow and alluvial sediments, while areas covered with regolith developed over the metamorphic basement are attributed to the low and very low groundwater potential zones. The GWPZI map will serve as a quick guide for effectively planning, managing, and developing the groundwater resources of the catchment.

1. Introduction

Most arid and semiarid climate regions in the world underlain by hard rocks face severe water shortages as a result of their physiographic conditions, which are exacerbated by climate change (Ahmed et al. 2007), and groundwater extraction has become an immediate alternative (Fenta et al. 2015). Although the Ethiopian highlands are major sources of recharge to the transboundary aquifers (TBAs) such as the Bulal catchment and have a significant distribution of the spatiotemporal potential of groundwater, access to fresh water is a challenge in the drought-prone peripheral regions (Alemayehu 2006, 2010; Moges 2012). Groundwater is a vital resource that provides more than 80% of the domestic and irrigation uses of Ethiopia (Kebede et al. 2005; Khadim et al. 2020). It is also often considered a reliable, drought-resilient resource (Calow et al. 1997; Taylor et al. 2013) that exists in all geological formations (Legesse and Ayenew 2006; Ayenew et al. 2008; Alemayehu et al. 2017; Kebede 2017). It ensures livelihood, especially in the southern parts of the country with prevailing semiarid climatic conditions where severe drought is common (Mera 2018; Razak et al. 2020).

The Bulal catchment underlain by volcanic and crystalline TBAs shared between Ethiopia and Kenya (Kebede et al. 2010; Razak et al. 2020) is among the 7 identified major TBAs of Ethiopia (IGRAC and UNESCO-IHP 2015). This work focuses only on the aquifers within the Ethiopian boundary. The Bulal catchment is characterized by semiarid climate, which receives low annual rainfall (Razak et al. 2020) and has been severely affected by drought in recent decades (Mera 2018). As a result, intermittent rivers/streams and lowered groundwater levels are common phenomena in the catchment (Razak et al. 2020). The Bulal catchment is mainly overlain by metamorphic basement complexes in the eastern part, Quaternary rift volcanic rocka in the southern part, and Neogene pre-rift volcanic rocks in the western part covered by thick layers of recent superficial deposits in places (Razak et al. 2020; Gebeyehu et al. 2022). The groundwater is confined in three major aquifer domains: 1) Quaternary sediments; 2) Borena basement, and 3) Bulal volcanic rocks (Kebede et al. 2010).

The groundwater resource potential of the TBAs in a water-stressed environment must be systematically evaluated and properly monitored in order to manage groundwater depletion problems and the impacts of climate change (Alemayehu 2010; Adiat et al. 2012; Hasheimi et al. 2015). Therefore, identifying groundwater potential zones is important. Although this could be better achieved through conventional approaches (i.e., geological, geophysical, hydrogeological surveys, borehole drilling and consequent pumping tests), they are costly and time-consuming compared to modern GIS and remote sensing (RS) techniques (Diwakar and Thakur 2012). Conventional exploration methods may not also be very reliable because they do not combine factors that influence the occurrence and movement of groundwater (Vidhya and Vinay 2019). However, an integrated application of GIS and RS is widely used as an efficient and cost-effective tool for delineating potential groundwater areas, especially in a semiarid environment (Sharma 2016). This method integrates multiple geo-environmental and hydrogeological parameters (Srivastava and Bhattacharya 2006; Jha et al. 2010; Dar et al. 2011; Singh et al. 2011a). The method has been proven to be an important tool for preparing thematic maps and conducting multi-criteria analysis (Vittala et al. 2005; Madrucci et al. 2008; Chowdhury et al. 2009; Javed and Wani 2009; Dar et al. 2010; Jha et al. 2010).

The aim of this research was to identify and delineate the groundwater potential zones of the catchment using an integrated application of GIS and RS in combination with Saaty's Analytical Hierarchal Process (AHP) (Saaty 1980, 1990). Ten thematic map layers that have significance for groundwater occurrences have been used and integrated by using GIS-overlay analysis to produce the groundwater potential zone index (GWPZI) map. The method is considered effective in identifying shallow to moderately deep groundwater zones. Subsequently, the results should be verified with ground field checks. However, data obtained from detailed geological, hydrogeological, and geophysical field investigations from 2010 to 2017 (OWWDSE 2017), and again in 2022, as well as from test wells, were utilized to validate the precision of the current GWPZI map output. The results of this study could serve as a quick guide and framework for policy- and decision-makers for developing sustainable groundwater resource studies, development, and management plans.

2. The Study Area

2.1. Location

The Bulal catchment is located in southern Ethiopia within the Borena Zone, Oromia regional state straddling the Ethiopia-Kenya border (Fig. 1). It covers an area of 14,641 km^2. The catchment can be accessed by a 464 km main asphalt road from Addis Ababa, the capital of Ethiopia, through Bule Hora and Yabelo towns. Several all-weather and dry-weather roads are also available for intersite mobilization.

[Insert Fig. 1 here]

2.2. Climate and topography

The Bulal catchment is characterized by an arid to semiarid climate with relatively high temperatures throughout the year with mean monthly maximum and minimum temperatures of 26°C and 15°C, respectively, and a mean annual temperature of 20.2°C. The rainfall pattern is characterized by two dry seasons (from December to February and July to August) and two rainy seasons, March to May and September to November. The mean annual rainfall in the catchment is ~ 608 mm (NMSA 2021).

The Bulal catchment is part of the Main Ethiopian Rift (MER) forming a topography reflecting volcano-tectonic activity. A flat to gently rolling terrain characterizes a substantial portion of the catchment area with a slope gradient of less than 3°. The elevation ranges from 702 m a. s. l. in the south to 2482 m a. s. l. in the central-eastern parts of the catchment (Fig. 1). The catchment exhibits two distinct physiographic regions i.e., the eastern warped plateau and associated ridges, and the central-southern rift floor plain with some isolated hills and valleys (Fig. 1).

2.3. Geological and hydrogeological setting

Quaternary rift volcanic rocks are the main geological formations in the Bulal catchment occupying the central and southern regions (Gebeyehu et al. 2022). They consist mainly of basaltic agglomerates, scoria falls, lappili tuffs and associated pyroclastic rocks, as well as vesicular and massive basalts (Bulal basalts). The Bulal basalt dominates the volcanic sequences in the catchment, is a horizontally layered basaltic lava flow with an average thickness of 200 m. The pre-rift basaltic flows associated with minor felsic pyroclastic deposits, phonolites, trachytes, and rhyolites occupy a limited area on the western elevated ridges of the catchment (Razak et al. 2020; Gebeyehu et al. 2022). The basement complex terrain occupying the eastern and southeastern parts is underlain by Precambrian basement rocks of quartzo-feldspathic, layered, and granitic gneisses with few granitic intrusions. On the other hand, most low-lying areas of the catchment are covered by relatively thick layers of recent superficial deposits, which comprise alluvial and eluvial sediments, and weathered regolith developed over the crystalline basement rocks (Fig. 2).

The Bulal catchment is highly affected by NW–SE, N–S and E–W oriented lineaments and faults. The N–S oriented Ririba normal fault system is one of the major fault zones in the catchment which runs from north to south of the whole catchment (Fig. 2). These structures have significance in governing the groundwater occurrence and flows in the catchment (Razak et al. 2020). In addition, crater maars and alluvial fans are common.

[Insert Fig. 2 here]

The fractured and weathered Bulal basalt is the major TBA unit in the catchment (Aquifer class I) (Kebede et al. 2010; Razak et al. 2020; Gebeyehu et al. 2022). Gebeyehu et al. (2022) indicated that this hydrostratigraphic unit is highly permeable and productive with average hydraulic conductivity (K) and transmissivity (T) values of 13 m/d and 642 m^2/d, respectively. Its average saturated thickness is ~ 70 m. Localized fractured and weathered basaltic aquifers intercalated with acidic volcanics (Aquifer class II) exhibit moderate productivity with average K and T values of 1 m/d and 115 m^2/d, respectively. Intergranular alluvial sediments and alluvial fans (Aquifer class III) over a limited area have a high storage potential for the underlying basaltic aquifer and moderate shallow groundwater productivity. A borehole drilled through this aquifer in the north yields ~ 9 l/s. An extensive intergranular hydrostratigraphic unit of unwelded pyroclastic deposits and regolith (Aquifer class IV), and weathered and fractured crystalline basement aquifers (Aquifer class V) act as local aquicludes and leaky aquifers with limited productivity where there are interconnected fractures (Fig. 3).

The deeper groundwater system of the Bulal catchment occurs under confined and semi-confined conditions mainly within the fractured zones of the Bulal basaltic aquifers (Kebede et al. 2010). The groundwater flow system in this aquifer media is dominantly discrete and fracture-controlled, and the flow converges from the eastern, western, and northern highlands to the southern low-lying areas following the Ririba fault system (Kebede et al. 2010; Razak et al. 2020; Gebeyehu et al. 2022). On the other hand, shallow groundwater confined to the upper thick unconsolidated sediments and regolith, has very short but continuous flow paths. Recharge mainly takes place from floods as diffuse recharge along the Ririba fault system and the Mega fault belt. Direct recharge from rainfall is very limited. The average annual recharge of the catchment estimated by a water balance model is 54 mm/year (Kebede et al. 2010; Razak et al. 2020), while it varies between 30 mm/year and 45 mm/year as estimated by the chloride-mass balance (CMB) method (Kebede et al. 2010).

[Insert Fig. 2 here]

3. Methodology

The delineation of the groundwater potential zones in the Bulal catchment was performed using a GIS-based overlay analysis technique. The overlay analysis was carried out by integrating ten thematic input layers that are important for groundwater occurrence and movement. Input layers include geology, groundwater level, soil texture, and lineament density, and remote sensing-derived data for land use/land cover (LULC), rainfall, drainage density, slope, topographic wetness index, and topographic variability. All the maps were prepared using the ArcGIS 10.8 platform and presented in UTM projection, zone 37 with reference datum of WGS84. All input raster layers were resampled to 100 m cell size resolution based on Tobler's rule (Tobler 1987) by taking the output map scale (1:250,000) into consideration. Saaty's AHP as a Multi-Criteria Decision-Making (MCDM) tool was used to assign the normalized weights to all input layers and their respective classes based on their relative influence on groundwater occurrence.

3.1. Selection of the input layers and their importance

To delineate the groundwater potential zones of the catchment, the major controlling factors of groundwater movement, storage, and occurrence should be investigated and identified (Kolli et al. 2020; Tolche 2021). The selection of the input layers for groundwater potential zone mapping was achieved by taking into consideration the relative influence of the input parameters on the groundwater occurrence, data availability, and the semiarid nature of the catchment (Razandi et al. 2014). The occurrence, movement, quality, and quantity of groundwater, particularly in semiarid areas, are governed by factors such as the underlying rock formations and their structural fabric, the thickness of weathered material, the topography, and climatic conditions (Thakur et al. 2011; Singh et al. 2011b; Gintamo 2015). Accordingly, ten (10) parameters were used. Geology (GG), lineament density (LD), land use/land cover (LULC), slope (SL),

topographic variability (TV), depth to groundwater (GD), rainfall (RF), drainage density (DD), soil texture (ST), and topographic wetness index (TWI) were selected and integrated to produce the GWPZI map of the catchment.

The geology of an area is one of the major factors that can affect the occurrence, movement, and quality of groundwater (Janardhana and Reddy 1998). It can determine the groundwater storage aquifer media and has a significant impact on groundwater recharge conditions (Shaban et al. 2006). Lineaments such as joints, fractures, and faults are straight to curvilinear geological discontinuities that are widely used in groundwater investigations to locate groundwater prospect sites on fractured bedrock (Edet et al. 1998; Sankar 2002). They may act as conduits for groundwater movement and storage, leading to increased secondary porosity and, therefore, can serve as groundwater potential zones (Rao 2006; Prasad et al. 2008; Idris et al. 2018). They can also influence the hydraulic properties (i.e., transmissivity, hydraulic conductivity, storativity, etc.) of the geological formations (Idris et al. 2018). Therefore, the connectivity and density of fractures/lineaments are significant determining factors for groundwater occurrence, storage, and flow of catchments such as Bulal, which are underlain by hard rocks (Idris et al. 2018).

Land use/land cover (LULC) is another important factor governing groundwater storage and recharge in a catchment (Singh 2013). It can influence the groundwater recharge and soil moisture of the region (Verma and Patel 2021).

Soil texture generally has a significant role in controlling the amount and rate of infiltrating water and recharge. The rate of infiltration largely depends on the grain size and permeability of the soils (Jasrotia et al. 2016).

Topographic variability controls groundwater subsurface movement, as elevation variation affects hydrological processes and the occurrence of groundwater potential (Muralitharan and Palanivel 2015; Kumar and Krishna 2018; Pourghasemi et al. 2020). The occurrence and flow of groundwater are also strongly governed by the slope gradient (Yeh et al. 2016). It has a strong effect on the infiltration of surface water and surface runoff depending on the slope variations, which in turn controls the groundwater recharge (Strahler 1964; Rajaveni et al. 2015). Furthermore, the topographic wetness index (TWI) plays an important role in the occurrence and development of groundwater. The TWI has been widely used to quantify topographical controls on hydrological processes and groundwater outflow to the surface (Beven and Kirkby 1979).

Precipitation in arid and semiarid regions is one of the major input parameters in determining the availability of groundwater recharge for aquifers (Thomas and Duraisamy 2018; Khan et al. 2022). The amount of recharge varies with the amount and intensity of rainfall (Verma and Patel 2021).

Drainage density is a function of exposed rock permeability. In areas covered with a low permeability rock, the drainage density is likely to be high, which in turn leads to low infiltration and greater runoff (Basavaraj Hutti and Nijagunappa 2020; Verma and Patel 2021). The depth to the groundwater level, on the other hand, is an important indicator of the existence and sustainability of groundwater resources in arid and semiarid regions. Seasonal groundwater level fluctuation in shallow aquifer systems of semiarid regions depends primarily on groundwater discharges, recharge, and the rate of evapotranspiration (Pavelic et al. 2012; Jhariya et al. 2016).

3.2. Data acquisition and preparation of the thematic layers

A geological map of the catchment area at the scale of 1:250,000 was obtained from the Oromia water works, design, and supervision enterprise (OWWDSE). It was modified and further reclassified into four major lithological units by taking their hydrogeological significance into consideration (Gebeyehu et al. 2022). Digital lineament features extracted manually from Sentinel-2 images were also obtained. Subsequently, the lineament density map layer was computed using a GIS algorithm with a 3 km buffer radius, which is expressed in terms of the total length of lineament per unit area (km/km^2) as expressed in Eq. 1 (Yeh et al. 2016).

$$\mathrm{L_d} = \frac{\sum_{i=1}^{i=n} \mathrm{L_i}}{\mathrm{A}} (1)$$

where, $\sum_{i=1}^{i=n} \mathrm{L_i}$represents the total length of lineaments (L) and A represents a unit area (L^2).

A vector data set of the land use/land cover (LULC) and soil maps of the catchment area prepared by OWWDSE at the scale of 1:50,000 (OWWDSE 2010) were used and converted into raster format in a 100 m cell size resolution in ArcGIS 10.8. The 2014 Shuttle Radar Topography Mission (SRTM) Digital Elevation Model (DEM) at 30 m resolution was used to produce thematic topographic variability and slope maps. The DEM was first gap-filled and resampled to a cell size of 100 m. In addition, the topographic wetness index (TWI) was prepared from the slope (in degrees), and the flow direction and flow accumulation input raster maps that were generated from the gap-filled DEM. Subsequently, the TWI was estimated and prepared in a GIS environment by means of a "TOPMODEL" simulation as expressed in Eq. 2 (Beven 1997).

$$\mathrm{TWI} = \ln \frac{\alpha}{\tan \beta} (2)$$

where, α = Upslope contributing area and β = topographic gradient (slope).

CHIRPS' monthly precipitation data for 22 years (1999–2021) were downloaded from the United States Geological Survey (USGS) website (https://chc.ucsb.edu/). The remotely sensed rainfall data were calibrated using data collected by the National Meteorological Service Agency (NMSA) at four stations (i.e., Mega, Moyale, Teltele, and Yabelo). Then, the point data were interpolated using the inverse distance weighted (IDW) tool in the GIS environment to produce the mean annual rainfall map layer. Drainage of the catchment area was first generated from a gap-filled DEM (30 m), and subsequently, the drainage density map (DD) was produced by using a line density algorithm in ArcGIS 10.8. The DD is expressed in terms of the length of channels per unit

area (km/km^2). Finally, average values of water level data from 69 wells, including 13 springs measured during both dry and wet seasons from the 2008 to 2017 period, were interpolated with IDW in ArcGIS 10.8 to produce the groundwater depth map of the Bulal catchment.

3.3. Weight assignment for the thematic layers

Appropriate weights were assigned to the ten input themes and their individual features after determining their relative importance in causing groundwater occurrence and movement in the Bulal catchment. The normalized weights of the individual themes and their different feature classes were obtained through Saaty's AHP approach (Saaty 1980, 1990). AHP as an MCDM tool was first introduced by Saaty in 1980. It has been widely used and successfully applied in groundwater potential mapping of arid and semiarid regions in particular (Machiwal et al. 2011; Kaliraj et al. 2014; Mallick et al. 2015; Rahaman et al. 2015; Ouma and Tateishi 2014). AHP is an efficient group decision-making technique that allows users to assess the relative importance of input parameters based on their experiences (Saaty 1999; Chowdhury et al. 2009). The Eigen normalized weights were employed for the ten input themes and their associated features in accordance with Saaty's 1–9 scale of assignment (Saaty 1980, 1990), which depicts the relative importance of each theme to groundwater availability (Tables 1 to 4). For computation of the Eigen normalized weights, open source Excel-based software version 15.09 of Goepel (2018) was used. Accordingly, geology (GG) was ranked as the dominant factor with a normalized weight of 0.265, while TWI was the least accounted for parameter with a normalized weight of 0.013 for groundwater occurrence in the catchment (Tables 2 to 4).

Table 1
Saaty's scale of relative importance for weight assignment (Saaty 1980, 1990).

Less important				**Equally important**	**More important**			
Extremely	Very Strongly	Strongly	Moderately	Equally	Moderately	Strongly	Very Strongly	Extremely
1/9	1/7	1/5	1/3	1	3	5	7	9
2, 4, 6 and 8 are intermediate values between the two adjacent judgments								

Table 2
Assigned and normalized weights of the ten thematic layers for groundwater potential zoning.

Theme	**Assigned Weight**	**Normalized weight**
Geology/Grouped Lithology (GG)	9	0.265
Lineament density (LD)	9	0.203
Land use/Land cover (LULC)	8	0.155
Rainfall (RF)	7	0.107
Slope (SL)	8	0.087
Topographic Variability (TV)	7	0.070
Depth to Groundwater (GD)	7	0.059
Drainage Density (DD)	2	0.022
Soil Texture (ST)	4	0.019
Topographic Wetness Index (TWI)	1	0.013

Table 3
Normalized weights and pair-wise comparison matrix of the ten thematic layers.

Theme	**GG**	**LD**	**LULC**	**RF**	**SL**	**TV**	**GD**	**DD**	**ST**	**TWI**	**Eigen normalized weight**
GG	1	1	3	3	5	7	5	9	8	9	0.265
LD	1	1	2	2	3	5	3	9	8	9	0.203
LULC	1/3	1/2	1	2	3	3	5	7	7	8	0.155
RF	1/3	1/2	1/2	1	3	2	2	5	5	7	0.107
SL	1/5	1/3	1/3	1/3	1	2	3	5	7	8	0.087
TV	1/7	1/5	1/3	1/2	1/2	1	3	5	5	7	0.070
GD	1/5	1/3	1/5	1/2	1/3	1/3	1	5	7	7	0.059
DD	1/9	1/9	1/7	1/5	1/5	1/5	1/5	1	3	2	0.022
ST	1/8	1/8	1/7	1/5	1/7	1/5	1/7	1/3	1	4	0.019
TWI	1/9	1/9	1/8	1/7	1/8	1/7	1/7	1/2	1/4	1	0.013

Table 4
Normalized weights for the subclasses of the ten thematic layers for groundwater potential zoning.

Theme	Sub-class	Groundwater prospect	Rank/ Assigned weight	CR	Normalized weight	
					Sub-class	Theme
Geology/ Grouped Lithology, 'GG'	Basalts associated with minor scoria and trachybasalts covered by thin eluvial deposits	Very high	8	0.03	0.536	0.265
	Recent deposits of alluvial and alluvial fans	High	4		0.283	
	Felsic volcanic rocks of rhyolites and trachytes associated with unwelded pyroclastic deposits of tuff and ash, and minor basalts	Moderate	3		0.123	
	Crystalline basement rocks covered by weathered regolith	Low	1		0.058	
Lineament Density, 'LD' (Km/Km^2)	0–0.26	Low	1	0.02	0.09	0.203
	0.27–0.49	Moderate	2		0.156	
	0.5–0.77	High	3		0.294	
	0.78–1.49	Very high	4		0.462	
Land use/ Land cover, 'LULC'	Dense Forest/woodland	Very high	9	0.05	0.274	0.155
	Dense Bushes/Shrubs	Very high	9		0.252	
	Open Vegetation/Trees	High	8		0.140	
	Open Bush/Shrub Land	High	8		0.105	
	Open Grass Land	Moderate	7		0.079	
	Cultivated Land	Moderate	7		0.054	
	Bare Land	Low	6		0.038	
	Marshy Area	Low	5		0.029	
	Rocky Surface	Very low	3		0.017	
	Settlement	Low	1		0.012	
Annual Rainfall, 'RF' (mm/year)	359–472	Low	1	0.02	0.09	0.107
	473–586	Moderate	2		0.156	
	587–690	High	3		0.294	
	691–858	Very high	4		0.462	
Slope, 'SL' (%)	< 2 (Flat)	Very high	9	0.02	0.474	0.087
	3–7 (Gentle)	High	8		0.317	
	8–15 (Sloping)	Moderate	3		0.107	
	16–30 (Moderately Steep)	Low	2		0.063	
	> 31 (Very Steep)	Very low	1		0.039	
Topographic Variability, 'TV' (m a. s. l.)	702–800 (Lowlands)	Very high	5	0.03	0.481	0.070
	801–1,250 (Plains)	High	3		0.405	
	1,251–1,650 (Uplands)	Low	1		0.114	
	1,651–2,482 (Inselbergs)	None	0		0	
Depth to Groundwater Level, 'GD' (m b. g. l.)	< 39	Low	1	0.02	0.09	0.059
	40–72	Moderate	2		0.156	
	73–104	High	3		0.294	
	> 105	Very high	4		0.462	
Drainage Density, 'DD' (km/km^2)	0.0006–0.0011	Low	1	0.02	0.09	0.022
	0.0004–0.0005	Moderate	2		0.156	
	0.0002–0.0003	High	3		0.294	
	0–0.0001	Very high	4		0.462	

Soil Texture (ST)	Sandy Loam	Very high	9	0.06	0.364	0.019
	Loam-Sand	Very high	9		0.274	
	Sandy Clay Loam	High	8		0.148	
	Loam	Moderate	7		0.098	
	Clayey Loam	Low	5		0.058	
	Clay	Low	5		0.039	
	Rocky Surface	Very Low	1		0.019	
Topographic Wetness Index, 'TWI'	4–7.9	Low	1	0.02	0.09	0.013
	8–9.9	Moderate	2		0.156	
	10–12.1	High	3		0.294	
	12.2–20	Very high	4		0.462	

The consistency index (CI) of the assigned weights was also calculated following the procedure suggested by Saaty (1990). The consistency ratio (CR), which indicates the probability that the matrix ratings were randomly generated was also computed using the following relations (Eq. 3 and Eq. 4):

$$\mathrm{CI} = (\lambda_{\max}) / (\mathrm{n} - 1) \, (3)$$

$$\mathrm{CR} = \mathrm{CI}/\mathrm{RI} \, (4)$$

where, λ_{max} is the principal eigenvalue, n is the number of criteria or factors, and RI is random consistence index.

For this study, the CR for assignments of the normalized weights to all input parameters was estimated to be 0.07 which is below the threshold consistency value of 0.1 (Saaty 1990). The CR values computed for each sub-classes of the theme are shown in Table 4.

3.4. Integration of the thematic layers using a weighted GIS-overlay analysis

All ten normalized weighted thematic layers were integrated using a sum-weighted overlay analysis tool on the GIS platform to demarcate the groundwater potential zones (GWPZs) of the Bulal catchment. The detailed procedures adopted for the delineation of GWPZ are shown as a flow chart in Fig. 4.

The integration of the normalized weighted input parameters to generate a composite GWPZI map of the catchment area was conducted using the procedure stated in Eq. 5.

$$\mathrm{GWPZI} = \mathrm{GG_w GG_{wi}} + \mathrm{LD_w LD_{wi}} + \mathrm{LULC_w LULC_{wi}} + \mathrm{RF_w RF_{wi}} + \mathrm{SL_w SL_{wi}} + \mathrm{TV_w GM_{wi}} + \mathrm{GD_w GD_{wi}} + \mathrm{DD_w DD_{wi}} + \mathrm{ST_w ST_{wi}} + \mathrm{TW}$$

Where, GG is the geology, LD is lineament density, LULC is land use/land cover, SL is slope, TV is topographic variability, GD is depth to groundwater, RF is rainfall, DD is drainage density, ST is soil texture and TWI is topographic wetness index, while w is normalized weight of the theme and wi (i = 1 to n) is normalized weight of subclass.

The final GWPZI map was further classified into four classes, i.e., 'high', 'moderate', 'low' and 'very low' potential zones based on the obtained index values from the combined impacts of the input parameters on the groundwater prevalence, employing a natural breaks method in ArcGIS 10.8 platform.

[Insert Fig. 4 here]

3.5. Validation and sensitivity analysis of the GWPZI map

A total of 40 wells with yield information were collated from previous studies by OWWDSE (2017). These yield data were used to check the accuracy of the classified GWPZI map of the catchment. In addition, sensitivity analysis (SA) was performed to determine the influence of each input parameter on the GWPZ output model using a map-removal technique (Lodwick et al. 1990). Accordingly, one input layer was removed at a time while the remaining parameters were calculated by using Eq. 6. The obtained sensitivity index (SI) values were then used to assess the impact of the removed layer in delineating the catchment area's the GWPZ map.

$$\mathrm{SI} = [[(\mathrm{GWPI}/\mathrm{N}) - (\mathrm{GWPI}\prime/\mathrm{n})] / \mathrm{GWPI}] * 100 \, (6)$$

where, SI = sensitivity index of the removed parameter/layer, GWPI = the groundwater potential index calculated using all input layers, GWPI' = the groundwater potential index obtained by excluding each input parameter at a time, and N and n are the numbers of input parameters used to delineate GWPZ and GWPZ', respectively.

A removed input layer with the highest SI indicates the most sensitive parameter while a parameter with the lowest SI is considered the least sensitive layer in delineating the GWPZI map of the catchment.

4. Results

4.1. Thematic map layers

4.1.1. Grouped geology/lithology (GG)

In general, the Bulal catchment is overlain by the transboundary Borena basement complex in the eastern region, while volcanic terrain occupies the western, central and southern parts of the catchment (see Fig. 2). The Quaternary Bulal basalt dominates the rift volcanics covering an extensive area of the catchment. It is also a major transboundary lithological unit that extends beyond the border to the Kenyan side (Kebede et al. 2010; Razak et al. 2020).

The lithological units in the catchment are further classified into four major groups based on their hydraulic properties, which affect their relative hydrogeological importance and productivity (Fig. 5a and Table 4): (i) Bulal basaltic flow; (ii) alluvial deposits; (iii) felsic volcanics; and (iv) crystalline basement rocks and associated regolith.

The Bulal basalt is mainly characterized by scoriaceous, vesiculated, and highly fractured lava flows. The fractures are highly penetrative and interconnected throughout the basaltic unit which favors groundwater circulation and storage in most places. However, the vesicles and fractures of the basalt at places are filled with secondary minerals (i.e., calcite and zeolites), and impervious weathered clay or laterites which may hinder groundwater movement and limit its productivity. Based on its high permeability and productivity, a higher normalized weight (0.54) was assigned to this unit (Fig. 5a and see Table 4). The recent superficial alluvial sediments and fans occupy limited areas in the northern and eastern regions, at the foot of hills and rift scarps. The sediment is dominantly composed of highly porous gravel and sand. This lithological unit is more than 80 m thick and has a high groundwater storage potential for the underlying basaltic rocks. It is also highly productive and favorable for shallow groundwater development. Accordingly, a weight of 0.28 was given to this unit (Fig. 5a and Table 4).

The pre-rift volcanics occupying the western elevated ridges and hills, and the Quaternary volcanics in most of the southern low-lying areas are mainly composed of acidic rocks of trachytes and rhyolites associated with pyroclastic deposits and minor basalts. The groundwater potential in the fractured and weathered sections of the acidic and basaltic rocks is relatively high. However, the presence of interlayered impervious pyroclastic falls and deposits may decrease their permeability, and as they occupy elevated grounds, they may act as local barriers to groundwater flow, which can limit their productivity in most places. Therefore, a moderate normalized weight of 0.12 was assigned to this unit.

The metamorphic basement rocks of various gneissic and granitic rocks are mostly outcrop along the eastern peripheral regions of the catchment. They have relatively little hydrogeological importance and influence on the groundwater availability except where they develop secondary porosity through fractures/joints and on thick weathered regolith deposits. Because of their low productivity and groundwater prospect, a lower weight of 0.06 was assigned to this unit (Fig. 5a and Table 4).

[Insert Fig. 5 here]

4.1.2. Lineament density (LD)

The Bulal catchment area is highly affected by lineaments and/or fractures because of rift-forming volcano-tectonic activities. NW–SE- and N–S-trending lineaments are prominent in the study area. The lineament density (LD) in the catchment varies between 0 and 1.5 km/km^2 (Fig. 5b and Table 4). For most of the catchment area, the LD is high, varying from 0.5 to 1.5 km/km^2. Although the lineaments are widespread across the catchment, the volcanic terrain has relatively higher LD than areas underlain by crystalline basement rocks. The localities with higher LD are regarded as having good prospects for groundwater storage and movement compared to those with the lowest LD. Accordingly, a higher weightage factor of 0.46 was assigned to localities with high LD and low normalized weight (0.09) to areas with low LD (Fig. 5b and Table 4).

4.1.3. Land use/land cover (LULC)

According to the LULC classification of the Bulal catchment, dense bushes and shrubs are the dominant types that cover most of the western, northern and southern parts followed by scattered bushes and shrubs (Fig. 5c and Table 4). Settlements, dense forest, rocky and marshy areas, and cultivated, grass and bare lands occupy very limited localities of the catchment. Together with the moderate annual precipitation (mean = 608 mm/year), the distribution of the LULC is expected to enhance the groundwater recharge depending on the underlying soil and geologic conditions. Accordingly, areas covered by dense vegetation of trees and shrubs were given the highest weights of 0.27 and 0.25, respectively (Fig. 5c and Table 4).

4.1.4. Rainfall (RF)

The mean annual rainfall of the Bulal catchment ranges from 359 to 858 mm/year. The western and eastern highlands receive a higher mean annual rainfall of 735 mm due to localized orographic effects, while the southern lowlands receive a mean annual rainfall of 468 mm/year (Fig. 5d and Table 4). Areas with high and moderate annual rainfall have weightage factors of 0.46 and 0.29, respectively signifying very good and moderate groundwater potential. On the other hand, areas with the lowest annual rainfall are given a 0.09 normalized weight, suggesting low groundwater potential.

4.1.5. Slope (SL)

The slope thematic layer (Fig. 5e) shows that the land gradient of the catchment varies between less than 2% and more than 31%. Most of the low-lying rift floor along the central and southern regions is characterized by flat to gently sloping land with slopes < 7%. On the other hand, the elevated areas with slope gradients > 16% (steep to very steep) constitute most of the western volcanic ridges and the northern and southeastern basement terrain. Accordingly, based on the land slope's influence on infiltration and groundwater recharge, areas with slopes of < 2% (i.e., nearly flat surfaces) were rated higher in terms of groundwater availability, and assigned a normalized weight of 0.47 compared to areas with slopes > 31% with weightage factor of 0.04 (Fig. 5e and Table 4).

4.1.6. Topographic variability (TV)

In the catchment area, four major topographic variability classes (landforms) were identified and demarcated based on their elevation variation and hydrogeological importance (Fig. 5f and Table 4). Most of the catchment is characterized by lowlands and plains with elevations ranging between 702 and 1250 m a. s. l. These landforms generally represent the low-lying rift floor covered by volcanic rocks and unconsolidated sediments. On the other hand, uplands and inselbergs representing the chain of high elevated ridge crests along the rift escarpment and hills constitute most of the northern and southeastern basement terrain. The plains and lowlands are the most favorable landforms for the occurrence of high groundwater potential and are subsequently assigned higher normalized weights (0.41 and 0.48, respectively). The uplands and inselbergs were given 0.11 and 0.0 weights, respectively, as they are considered to be unfavorable land features for the availability of groundwater potential and unsuitable for groundwater development.

4.1.7. Depth to groundwater level (GD)

The depth to groundwater level of the Bulal catchment varies between 0 and 159 m below ground level (b. g. l.) with a mean of 70 m b. g. l. (Fig. 6a and Table 4). The spatial map (Fig. 6a) indicates that the shallower groundwater system is mainly confined to the regolith developed over the basement rocks and unconsolidated sediments in the eastern parts, while the deeper groundwater is developed on the fractured basaltic rocks in the central parts of the catchment. Due to the arid condition of the catchment and high evapotranspiration, the shallow groundwater system tends to be vulnerable to seasonal water level fluctuations and yield deteriorations compared to the deeper groundwater system in volcanic rocks. Therefore, areas with shallow groundwater levels are considered unreliable and unfavorable groundwater potential zones and subsequently assigned the lowest weight (0.09) compared to the areas with deeper groundwater levels (0.46) (Fig. 6a and Table 4).

[Insert Fig. 6 here]

4.1.8. Drainage density (DD)

An area with a very high drainage density represents more closeness of drainage channels and high runoff, while a lower DD indicates lower run-off and a higher probability of recharge and groundwater potential. Most of the drainage originates from the volcanic ridges and inselbergs in the west, and the basement ridges in the northern and eastern parts of the catchment. Figure 6b shows that the DD of the catchment ranges from < 0.0001 to 0.0011 km/km^2. Areas with the highest DD are weighted relatively lower (0.09) compared to very low drainage density areas, which are given a high weightage factor (0.46). However, the generally moderate to high drainage density in the catchment implies low or moderate infiltration and recharge potentials.

4.1.9. Soil texture (ST)

Fine-grained soils limit infiltration due to their lower permeability, unlike coarse-grained soil materials where water can infiltrate easily because of high permeability. In this study, six major soil texture units were identified: clay, clayey loam, loam, sandy-clayey loam, loamy sand, and sandy loam (Fig. 6c and Table 4). As shown in Fig. 6c, sandy loam is the dominant soil texture covering an extensive area of the Bulal catchment. Due to its higher sand content (coarse grained materials) and permeability, a higher weightage factor was given to the sandy loam soil units (0.36) compared to areas covered by massive, unfractured rocks and clayey soil with a normalized weight of 0.02 and 0.04, respectively (Fig. 6c and Table 4).

4.1.10. Topographic wetness index (TWI)

In the catchment area, the TWI value varies between 4 and 20 with a mean of 9.5 (Fig. 6d and Table 4). The slightly elevated areas with gentle sloping drainage systems where runoff waters from the highlands accumulate have a relatively higher TWI value. On the other hand, the well-elevated areas with steep sloping drainages have relatively lower TWI or surface accumulation. Therefore, an area with a higher value of TWI has good prospects for groundwater occurrence and is assigned a high weight (0.46), whereas areas with the lowest TWI value are considered to be of low groundwater prospect and given a low weight of 0.095 (Fig. 6d and Table 4).

4.2. Sensitivity analysis of the GWPZI map

A sensitivity analysis was performed to determine the influence of each input parameter in delineating the GWPZ map of the Bulal catchment. Accordingly, the sensitivity index (SI) shows that geology (GG) with a mean SI value of 1.7% and topographic wetness index (TWI) with a mean of -1% are the most and least sensitive parameters in delineating the GWPZI map, respectively (Table 5). In other words, the geological layer has a significant impact on the spatial distributions of groundwater potentiality in the catchment. As a result, the removal of geology reduces the area coverage of the high and very low zones by ~ 7% each, while increasing the moderate zone by ~ 14%. The topographic wetness index is the least influential factor on the catchment's groundwater potential, and removing it from the delineation of the GWPZI map has no effect on the spatial extents of the potential zones (Table 5).

Table 5
Map-removal sensitivity analysis index for the GWPZI of the Bulal catchment.

Layer removed	Sensitivity variation index (SI) in %				Area of changed GWPZI' class (%)				Area difference (%) (GWPZI – GWPZI')			
	Min.	Max.	Mean	StD	High	Moderate	Low	Very low	High	Moderate	Low	Very low
Geology (GG)	-05	5.9	1.7	1.8	19.4	34.2	28.0	18.4	7.3	-14.0	0.0	6.7
Lineament density (LD)	-0.6	5.3	0.9	1.1	24.0	21.0	21.0	34.0	2.7	-0.8	7.0	-8.9
Land use/Land cover (LULC)	-1.0	2.5	0.2	0.6	21.8	22.7	27.5	28.0	4.9	-2.5	0.5	-2.9
Rainfall (RF)	-0.8	3.3	0.3	0.7	22.0	23.0	27.0	28.0	4.7	-2.8	1.0	-2.9
Slope (SL)	-1.0	2.2	0.3	0.7	28.6	21.0	28.2	22.2	-1.9	-0.8	-0.2	2.9
Topographic variability (TV)	-1.1	1.9	-0.1	0.5	27.6	20.0	27.6	24.8	-0.9	0.2	0.4	0.3
Depth to groundwater (GD)	-1.0	1.0	-0.5	0.3	25.0	21.3	27.0	26.7	1.7	-1.1	1.0	-1.6
Drainage density (DD)	-1.1	0.2	-0.8	0.2	27.7	19.6	27.5	25.2	-1.0	0.6	0.5	-0.1
Soil texture (ST)	-1.1	-0.4	-0.9	0.2	28.0	19.7	27.3	25.0	-1.3	0.5	0.7	0.1
Topographic wetness index (TWI)	-1.1	-0.6	-1.0	7.2	26.7	20.4	27.7	25.2	0.0	-0.2	0.3	-0.1

[Insert Table 5 here]

5. Discussion

5.1. Classification of groundwater potential zones

The GWPZI map of the Bulal catchment shows four distinct potential zones (i.e., very low, low, moderate and high) (Fig. 7 and Table 6). The potential map provides a quick perspective on the storage and availability of groundwater resources in the catchment. The GWPZI map indicates that the western and eastern peripheral regions have low to very low groundwater potential, while most of the northern, central and southern low-lying rift floor areas generally exhibit moderate to high potential. The map shows a highly productive deeper aquifer system of basaltic rocks, dominantly the Bulal basalts. Among the major lithologic units in the catchment, the Bulal basaltic flow overlain by thick sediments in places forms an extensive and highly to moderately productive major TBA system, as revealed by the GWPZI map (Fig. 7). The alluvial sediments in fans along the feet of rift scarps and ridges and the weathered regolith deposits over the crystalline basement also have the potential to store groundwater at shallow depths. Weathered and fractured acidic volcanic rocks can also form deeper potential aquifers along lineaments/fractures and fault lines. On the other hand, the low and very low GWP areas show limited aquifer capabilities of the metamorphic basement rocks associated with regolith and minor pyroclasts.

Table 6
Classification of groundwater potential zones along with their respective yield categories.

GWP Zones	Major Aquifer Units	Well yield (l/s)		Area	
		Q (Range)	Mean 'Q'	Km^2	%
High	Basalts (Bulal basalt) and alluvial deposits	8–71	25	3878.4	26.7
Moderate	Bulal basalt, felsic rocks and alluvial deposits	3.1–8.0	5.0	2929.6	20.2
Low	Regolith deposits developed over the basement	1–3	2.6	4053.8	28.0
Very Low	Metamorphic basement rocks overlain by regolith and unwelded acidic volcanics (pyroclastic deposits)	0.5–1.0	0.8	3643.6	25.1

The GWPZI map indicates that the distribution of groundwater potential is a function of the lithological input layer, while lineament density, slope, topographic variability, and groundwater depth also play a significant role. Areas underlain by the Bulal basaltic flows associated with acidic volcanics and alluvial sediments along the northern, western, central and southern parts forming plains with flat to gently rolling slopes, with high lineament density, and covered by bushes and shrubs have high to moderate groundwater potential. On the other hand, areas underlain by the metamorphic basement rocks covered by regolith deposits in the eastern part of the catchment forming rugged and highly elevated topography with relatively steep slopes, high drainage densities, low topographic wetness index, and lower lineament densities, exhibit very low to low shallow groundwater potential. Moreover, the predominantly ridge-forming, steeply sloped felsic rocks (trachytes and rhyolites) with minor basalts in the western part of the catchment show low to very low groundwater potential.

In short, high to moderate groundwater potential in the Bulal catchment is associated with a combination of the following factors: (i) fractured and weathered basaltic rocks, (ii) high lineament density, (iii) dense vegetation cover, and (iv) low gradient plains.

[Insert Fig. 7 here]

[Insert Table 6 here]

5.2. Validation of the GWPZI map

The accuracy of the GWPZI map was evaluated by superimposing yield data from 40 boreholes within the catchment. Well yields varying between 8 l/s and 71 l/s with a mean of 25 l/s and 3.1 l/s and 8 l/s with a mean of 5 l/s are attributed to the high and moderate potential zones, respectively. On the other hand, well yields varying from 1 l/s to 3 l/s (average 2.6 l/s) and yields below 1 l/s (average 0.8 l/s) fall in the low and very low potential zones, respectively (Fig. 7 and Table 6).

The well yields also show clustering with the lithologies (Fig. 8). Most wells with yields ≥ 8 l/s (high yield) are mainly on the Bulal basaltic flows and associated alluvial sediments. On the other hand, most wells within the regolith developed over the metamorphic basement, and pyroclastic deposits have low (1–3 l/s) and very low (≤ 1 l/s) yields. The moderate yield (3.1–8 l/s) wells mostly plot on the fractured basaltic and felsic rocks covered by some alluvial sediment. The well yield distribution very well validates the GWPZI map of the catchment.

The validation clearly justifies the efficiency of the integrated RS and GIS-based overlay analysis technique employed in the delineation of the groundwater potential zones. This technique is a useful modern approach for proper groundwater resource investigation and development. However, it should be noted that the developed GWPZI map can only provide a quick prospective guide for the purpose of regional groundwater exploration and development. Detailed ground-truthing and further verifications should be considered for site-specific groundwater investigation and development.

[Insert Fig. 8 here]

6. Conclusions

Using Saaty's AHP approach as an MCDM tool, a composite GWPZI map is produced and delineates the groundwater potential zones of the Bulal catchment. The work shows the following:

1. There are four groundwater potential zones in the catchment: high, moderate, low and very low. The high and moderate groundwater potential zones represent 27% and 20% of the total catchment area, respectively, while low and very low potential zones together account for approximately53% of the total area.
2. The geological (lithology, structure density) and geomorphological (topography, slope) features are the most dominant influencing factors in the distribution of groundwater potential in the catchment, as also shown by the sensitivity analysis, where geology is the most influencing factor while soil texture and topographic wetness index are the least sensitive.
3. Areas underlain by the transboundary Bulal basaltic rocks in most of the central and southern parts of the catchment are characterized by high to moderate groundwater potential zones, while areas with low and very low groundwater potential are typically associated with the regolith deposits over the metamorphic basement rocks in the eastern periphery of the catchment.
4. High to moderate groundwater potential zones are associated with a combination of the fractured and weathered basaltic rocks, high lineament density, dense vegetation cover, and low slope gradient.
5. The accuracy of the GWPZI map is well validated by the groundwater well yields from the catchment where areas with high and moderate groundwater potential are characterized by average well yields of 25 l/s and 5 l/s, respectively, while those with average yields of 2.6 l/s and 0.8 l/s represent low and very low potential zones, respectively.
6. The integrated RS and GIS-based overlay analysis technique used to delineate the groundwater potential zones is efficient and could be a useful technique for proper regional groundwater exploration and development.

Declarations

Declaration of competing interest

The authors declare that they have no known competing financial interests or personal relationships that could have appeared to influence the work reported in this paper.

Acknowledgements

This work is part of the PhD thesis of AG under the supervision of TA and AA. The Engineering Corporation of Oromia – ECO (formerly "Oromia Water Works, Design and Supervision Enterprise – OWWDSE"), National Meteorological Services Agency of Ethiopia (NMSA), and United States Geological Survey (USGS) are acknowledged for providing data and documentary resources.

Data availability statement

All relevant data are included in the paper. Readers should also contact the corresponding author for further details.

References

1. Adiat KAN, Nawawi MNM, Abdullah K (2012) Assessing the accuracy of GIS-based elementary multicriteria decision analysis as a spatial prediction tool – A case of predicting potential zones of sustainable groundwater resources. J. Hydrol. 440–441: 75–89. https://doi.org/10.1016/J.JHYDROL.2012.03.028.

2. Ahmed S, Maréchal JC, Ledoux E, De Marsily G (2007) Groundwater modeling in hard-rock terrain in semiarid areas: experience from India. Hydrological modelling of arid and semiarid areas. Cambridge, UK: Cambridge University Press: p157–190, doi:10.1017/CBO9780511535734.012.
3. Alemayehu T, Kebede S, Liu L, Kebede T (2017) Basin hydrogeological characterization using remote sensing, hydrogeochemical and isotope methods (the case of Baro-Akobo, Eastern Nile, Ethiopia). Environ. Earth Sci. 76: 466.
4. Alemayehu T (2010) An overview of the transboundary aquifers in East Africa. J. Afr. Earth Sci. 58 (4): 684–691. https://doi.org/10.1016/j.jafrearsci.2009.10.003.
5. Alemayehu T (2006) Groundwater Occurrence in Ethiopia; Addis Ababa University Press: Addis Ababa, Ethiopia. p105.
6. Ayenew T, Kebede S, Alemyahu T (2008) Environmental isotopes and hydrochemical study applied to surface water and groundwater interaction in the Awash River basin. Hydrol. Process. 22: 1548–1563.
7. Basavaraj Hutti, Nijagunappa R (2020) Development of Groundwater Potential Zone in North-Karnataka Semiarid Region Using Geoinformatics Technology. Uni. J. Environ. Res. and Technol. 1 (4): 509. https://www.environmentaljournal.org.
8. Beven K (1997) TOPMODEL: A critique. Hydrol. Process. 11: 1069–1085.
9. Beven KJ, Kirkby MJ (1979) A physically based, variable contributing area model of basin hydrology. Hydrol. Sci. Bull. 24: 43–69. https://doi.org/10.1080/02626667909491834.
10. Calow RC, Robins NS, MacDonald AM, MacDonald DM, Gibbs BR, Orpen WR, Mtembezeka P, Andrews AJ, Appiah SO (1997) Groundwater management in drought-prone areas of Africa. Int. J. Water Resour. Dev. 13: 241–62.
11. Chowdhury A, Jha MK, Chowdary VM, Mal BC (2009) Integrated remote sensing and GIS-based approach for assessing groundwater potential in West Medinipur district, West Bengal, India. Int. J. Remote. Sens. 30(1): 231–250. https://doi.org/10.1080/01431160802270131.
12. Dar IA, Sankar K, Dar MA (2011) Deciphering groundwater potential zones in hard rock terrain using geospatial technology. Environ. Monit. & Assess. 173 (1): 597–610.
13. Dar IA, Sankar K, Dar MA (2010) Remote Sensing Technology and Geographic Information System Modeling: An Integrated Approach towards the Mapping of Groundwater Potential Zones in Hardrock Terrain, Mamundiyar Basin. J. Hydrol. 394 (3–4): 285–295. doi:10.1016/j.jhydrol.2010.08.022.
14. Diwakar J, Thakur JK (2012) Environmental system analysis for river pollution control. Water, Air, & Soil Pollut. 223: 3207–3218. doi:10.1007/s11270-012-1102-z.
15. Edet AE, Okereke CS, Teme SC, Esu EO (1998) Application of remote-sensing data to groundwater exploration: a case study of the Cross River State, Southeastern Nigeria. Hydrogeol. J. 6(3): 394–404.
16. Fenta AA, Kifle A, Gebreyohannes T, Hailu G (2015) Spatial analysis of groundwater potential using remote sensing and GIS-based multi-criteria evaluation in Raya Valley, northern Ethiopia. Hydrogeol. J. 23: 195–206. https://doi.org/10.1007/s10040-014-1198-x.
17. Gebeyehu A, Ayenew T, Asrat A (2022) Hydrogeochemistry of the groundwater system of the transboundary basement and volcanic aquifers of the Bulal catchment, Southern Ethiopia. J. Afr. Earth Sci. 194 (104622): 1–2. https://doi.org/10.1016/j.jafrearsci.2022.104622.
18. Gintamo TT (2015) Ground Water Potential Evaluation Based on Integrated GIS and Remote Sensing Techniques, in Bilate River Catchment: South Rift Valley of Ethiopia. Am. Sci. Res. J. for Eng. Tech. & Sci. 10 (1): 85–120.
19. Goepel KD (2018) Implementing the Analytic Hierarchy Process as a Standard Method for Multi-Criteria Decision Making in Corporate Enterprises—A New web-based AHP Excel template software 15.09.2018 version with Multiple Inputs. California, USA. http://bpmsg.com
20. Hashemi H, Uvo CB, Berndtsson R (2015) Coupled modeling approach to assess climate change impacts on groundwater recharge and adaptation in arid areas. Hydrol. & Earth Syst. Sci.19 (10): 4165–4181. https://doi.org/10.5194/hess-19-4165.
21. Idris MA, Garba ML, Kasim SA, Madabo IM, Dandago KA (2018) The Role of Geological Structures on Groundwater Occurrence and Flow in Crystalline Basement Aquifers: A Status Review. Bayero J. Pure & Appl. Sci. 1(1): 155–164. http://dx.doi.org/10.4314/bajopas.v11i1.27.
22. IGRAC (International Groundwater Resources Assessment Centre), UNESCO-IHP (UNESCO International Hydrological Programme) (2015) Transboundary Aquifers of the World Map, 2015. Scale 1: 50,000,000. Delft, Netherlands.
23. Jasrotia AS, Kumar A, Singh R (2016) Integrated remote sensing and GIS approach for delineation of groundwater potential zones using aquifer parameters in Devak and Rui watershed of Jammu and Kashmir, India. Arab. J. Geosci. 9 (4): 1–15. https://doi.org/10.1007/s12517-016-2326-9.
24. Javed A, Wani MH (2009) Delineation of groundwater potential zones in Kakund watershed, Eastern Rajasthan, using remote sensing and GIS techniques. J. Geol Soc. India. 73:229–236.
25. Jha MK, Chowdary VM, Chowdhury A (2010) Groundwater Assessment in Salboni Block, West Bengal (India) Using Remote Sensing, Geographical Information System and Multi-Criteria Decision Analysis Techniques. Hydrogeol. J. 18(7):1713–1728.
26. Jhariya DC, Kumar T, Gobinath M, Diwan P, Kishore N (2016) Assessment of Groundwater Potential Zone Using Remote Sensing, GIS and Multi Criteria Decision Analysis Techniques. J. Geol. Soc. of India. 88 (4): 481–492.
27. Kaliraj S, Chandrasekar N, Magesh NS (2014) Identification of Potential Groundwater Recharge Zones in Vaigai Upper Basin, Tamil Nadu, Using GIS-Based Analytical Hierarchical Process (AHP) Technique. Arab. J. Geosci. 7: 1385–1401. https://doi.org/10.1007/s12517-013-0849-x.
28. Kebede S, Ketema A, Tesema Z (2010) Features of groundwaters in basins shared between Ethiopia and Kenya and the implications for international legislation on transboundary aquifers. Hydrogeol. J. 18: 1685–1697.
29. Kebede S, Travi Y, Alemayehu T, Ayenew T (2005) Groundwater recharge, circulation and geochemical evolution in the source region of the Blue Nile River, Ethiopia. Appl. Geochem. 20 (9): 1658–1676.

30. Khadim FK, Dokou Z, Lazin R, Moges S, Bagtzoglou AC, Anagnostou E (2020) Groundwater modeling in data scarce aquifers: The case of Gilgel-Abay, Upper Blue Nile, Ethiopia. J. Hydrol. 125214: 590.
31. Khan MYA, ElKashouty M, Tian F (2022) Mapping Groundwater Potential Zones Using Analytical Hierarchical Process and Multicriteria Evaluation in the Central Eastern Desert, Egypt. Water. 14 (1041): 7. https://doi.org/10.3390/w14071041.
32. Kolli M, Opp C, Groll M (2020) Mapping of potential groundwater recharge zones in the Kolleru Lake catchment, India, by using remote sensing and GIS techniques. Nat. Resour. 11: 127–145.
33. Kumar A, Krishna AP (2018) Assessment of groundwater potential zones in coal mining impacted hard-rock terrain of India by integrating geospatial and analytic hierarchy process (AHP) approach. Geocarto. Int. 33 (2): 105–129. https://doi.org/10.1080/10106049.2016.1232314.
34. Legesse D, Ayenew T (2006) Effect of improper water and land resource utilization on the central Main Ethiopian Rift lakes. Quat. Int. 148: 8–18.
35. Lodowik WA, Monson W, Svoboda L (1990) Attribute Error and Sensitivity Analysis of Map Operations in Geographical Information Systems: Suitability Analysis. Int. J. Geogr. Inf. Syst. 4(4): 413–428. Doi:10.1080/02693799008941556.
36. Machiwal D, Jha MK, Mal BC (2011) Assessment of groundwater potential in a semiarid region of India using remote sensing, GIS and MCDM techniques. Water Resour. Manag. 25(5): 1359–1386. https://doi.org/10.1007/s11269-010-9749-y.
37. Madrucci,V, Taioli F, de Araújo CC (2008) Groundwater favorability map using GIS multicriteria data analysis on crystalline terrain, Sao Paulo State, Brazil. J. Hydrol. 357: 153–173.
38. Mallick J, Singh CK,, Al-Wadi H, Ahmed M, Rahman A, Shashtri S, Mukherjee S (2015) Geospatial and Geostatistical Approach for Groundwater Potential Zone Delineation. Hydrol. Process. 29 (3): 395–418. https://doi.org/10.1002/hyp.10153.
39. Mera GA (2018) Drought and its impacts in Ethiopia. Weather. & Clim. Extrem. 22 (2018): 24–35. DOI: 10.1016/j.wace.2018.10.002.
40. Moges S (2012) AgWater Solutions Project Case Study Agricultural Use of Ground Water in Ethiopia: Assessment of Potential and Analysis of Economics, Policies, Constraints and Opportunities. Research Report. Gates Found. Open Res. p9–49. http://awm-solutions.iwmi.org/home-page.aspx.
41. Muralitharan, J, Palanivel K (2015) Groundwater targeting using remote sensing, geographical information system and analytical hierarchy process method in hard rock aquifer system, Karur district, Tamil Nadu, India. Earth Sci. Info., 8: 827–842. https://doi.org/10.1007/S12145-015-0213-7.
42. NMSA (2021). National Meteorological Services Agency, Addis Ababa, Ethiopia.
43. Oromia Water Works, Design and Supervision Enterprise (OWWDSE) (2017) Groundwater resources evaluation and assessment project of Borena area. Volume V: Hydrogeology & Groundwater Modeling, Annex- I: Hydrogeology main report (unpublished). p19–107.
44. Ouma YO, Tateishi R (2014) Urban Flood Vulnerability and Risk Mapping Using Integrated Multi-Parametric AHP and GIS: Methodological Overview and Case Study Assessment. Water. 6(6): 1515–1545. https://doi.org/10.3390/w6061515.
45. Pavelic P, Patankar U, Acharya S, Jella K, Gumma MK (2012) Role of groundwater in buffering irrigation production against climate variability at the basin scale in South-West India. Agric. Water Manage. 103:78–87.
46. Pourghasemi HR, Sadhasivam N, Yousef S, Tavangar S, Ghaffari Nazarlou H, Santosh M (2020) Using machine learning algorithms to map the groundwater recharge potential zones. J. Environ. Manag. 265: 110525. https://doi.org/10.1016/J.JENVMAN.2020.110525.
47. Prasad RK, Morrdal NC, Banerjee P, Nandakumar MV, Singh VS (2008) Deciphering potential groundwater zone in hard rock through the application of GIS. Environ. Geol. 55:467–475.
48. Rahaman SA, Ajeez SA, Aruchamy S, Jegankumar R (2015) Prioritization of Sub Watershed Based on Morphometric Characteristics Using Fuzzy Analytical Hierarchy Process and Geographical Information System—A Study of Kallar Watershed, Tamil Nadu. Aquat. Procedia. 4: 1322–1330. https://doi.org/10.1016/j.aqpro.2015.02.172.
49. Rajaveni S, Brindha K, Elango L (2015) Geological and geomorphological controls on groundwater occurrence in a hard rock region. Appl. Water Sci. 7: 1377–1389.
50. Rao NS (2006) Groundwater potential index in a crystalline terrain using remote sensing data. Environ. Geol. 50:1067–1076.
51. Razak M, Furi W, Fanta L, Shiferaw A (2020) Water Resource Assessment of a Complex Volcanic System under Semiarid Climate Using Numerical Modeling: The Borena Basin in Southern Ethiopia. Water. 12(276): 4–8. doi:10.3390/w12010276 www.mdpi.
52. Razandi Y, Pourghasemi HR, Neisani NS, Rahmati O (2014) Application of analytical hierarchy process, frequency ratio, and certainty factor models for groundwater potential mapping using GIS. Earth Sci. Inform. 8(4): 867–883.
53. Saaty T L (1999) Fundamentals of the analytic network process, International Symposium of the Analytic Hierarchy Process (ISAHP), Kobe, Japan.
54. Saaty TL (1990) How to make a decision: The analytic hierarchy process. Eur. J. Oper. Res. 48 (1): 9–26. https://doi.org/10.1016/0377-2217(90)90057-I.
55. Saaty TL (1980) The analytic hierarchy process: planning, priority setting, resource allocation. McGraw-Hill, New York. p340.
56. Sankar K (2002) Evaluation of Groundwater Potential Zones Using Remote Sensing Data In Upper Vaigai River Basin, Tamil Nadu, India. J. Indian Soc. Remote. Sens. 30(3): 119–129.
57. Shaban A, Khawlie M, Abdallah C (2006) Use of Remote Sensing and GIS to Determine Recharge Potential Zones: The Case of Occidental Lebanon. Hydrogeol. J. 14(4): 433–443. DOI: 10.1007/s10040-005-0437-6.
58. Sharma RS (2016) Identification of Groundwater recharge potential zones in Thiruverumbur block, Trichy district using GIS and remote sensing. Int. J. Geoinform. & Geol. Sci. 3(2): 6–11.
59. Singh AK, Panda SN, Kumar KS, Sharma S (2013) Artificial groundwater recharge zones mapping using remote sensing and GIS: a case study in Indian Punjab. Environ. Manag. 52: 61–71.

60. Singh PK, Thakur JK, Kumar S, Singh UC (2011a) Assessment of land use/land cover using geospatial techniques in a semiarid region of Madhya Pradesh, India. Geospat. Tech. for manag. Environ. res. Heidelberg, Germany: 152–163. DOI 10.1007/978-94-007-1858-6_10.
61. Singh PK, Kumar S, Singh UC (2011b) Groundwater resource evaluation in the Gwalior area, India, using satellite data: an integrated geomorphological and geophysical approach. Hydrogeol. J. 1–9. doi:10.1007/s10040-10011-10758-10046.
62. Srivastava PK, Bhattacharya AK (2006) Groundwater assessment through an integrated approach using remote sensing, GIS and resistivity techniques: A case study from a hard rock terrain. Int. J. Remote. Sens. 27 (20): 4599–4620. https://doi.org/10.1080/01431160600554983.
63. Strahler AN (1964) Quantitative geomorphology of drainage basins and channel networks. In Handbook of Applied Hydrology; Chow, V.T., Ed.; McGraw Hill Book Company: New York, NY, USA: p4–11.
64. Taylor RG, Scanlon B, Döll P, Rodell M, Van Beek R, Wada Y, Longuevergne L, Leblanc M, Famiglietti JS, Edmunds M (2013) Ground water and climate change. Nat. Clim. Chang. 3: 322–329.
65. Thakur JK, Thakur RK, AL Ramanathan, Kumar M, Singh SK (2011) Arsenic contamination of groundwater in Nepal - an overview. Water. 3 (1): 1–20. doi:10.3390/w3010001.
66. Thomas R, Vijayasekaran Duraisamy V (2018) Hydrogeological delineation of groundwater vulnerability to droughts in semiarid areas of western Ahmednagar district. The Egypt. J. Remote. Sens. Space Sci. 21 (2): 121–137. https://doi.org/10.1016/j.ejrs.2016.11.008.
67. Tobler W (1987) Measuring Spatial Resolution Proposed to the conference on Land Use and Remote Sensing, Beijing. p12–16.
68. Tolche AD (2021) Groundwater potential mapping using geospatial techniques: A case study of Dhungeta-Ramis sub-basin, Ethiopia. Geol. Ecol. Landsc. 5: 65–80. https://doi.org/10.1080/24749508.2020.1728882.
69. USGS (2021) United States Geological Survey. CHIRPS' monthly series precipitation image data (1999–2021) available online: https://chc.ucsb.edu/ (accessed on 22 October 2021).
70. Verma N, Patel RK (2021) Delineation of groundwater potential zones in lower Rihand River Basin, India using geospatial techniques and AHP. Egypt. J. Remote. Sens. & Space Sci. 2–10. https://doi.org/10.1016/j.ejrs.2021.03.005.
71. Vidhya SL, Vinay YKR (2019) Identification of groundwater potential zones using GIS and remote sensing. Int. J. Pure & Appl. Math. 119 (17): 3195–3210. http://www.acadpubl.eu/hub/.
72. Yeh HF, Cheng YS, Lin HI, Lee CH (2016) Mapping groundwater recharge potential zone using a GIS approach in Hualian River, Taiwan. Sustain. Environ. Res. 26(1): 33–43. https://doi.org/10.1016/j.serj.2015.09.005.

Figures

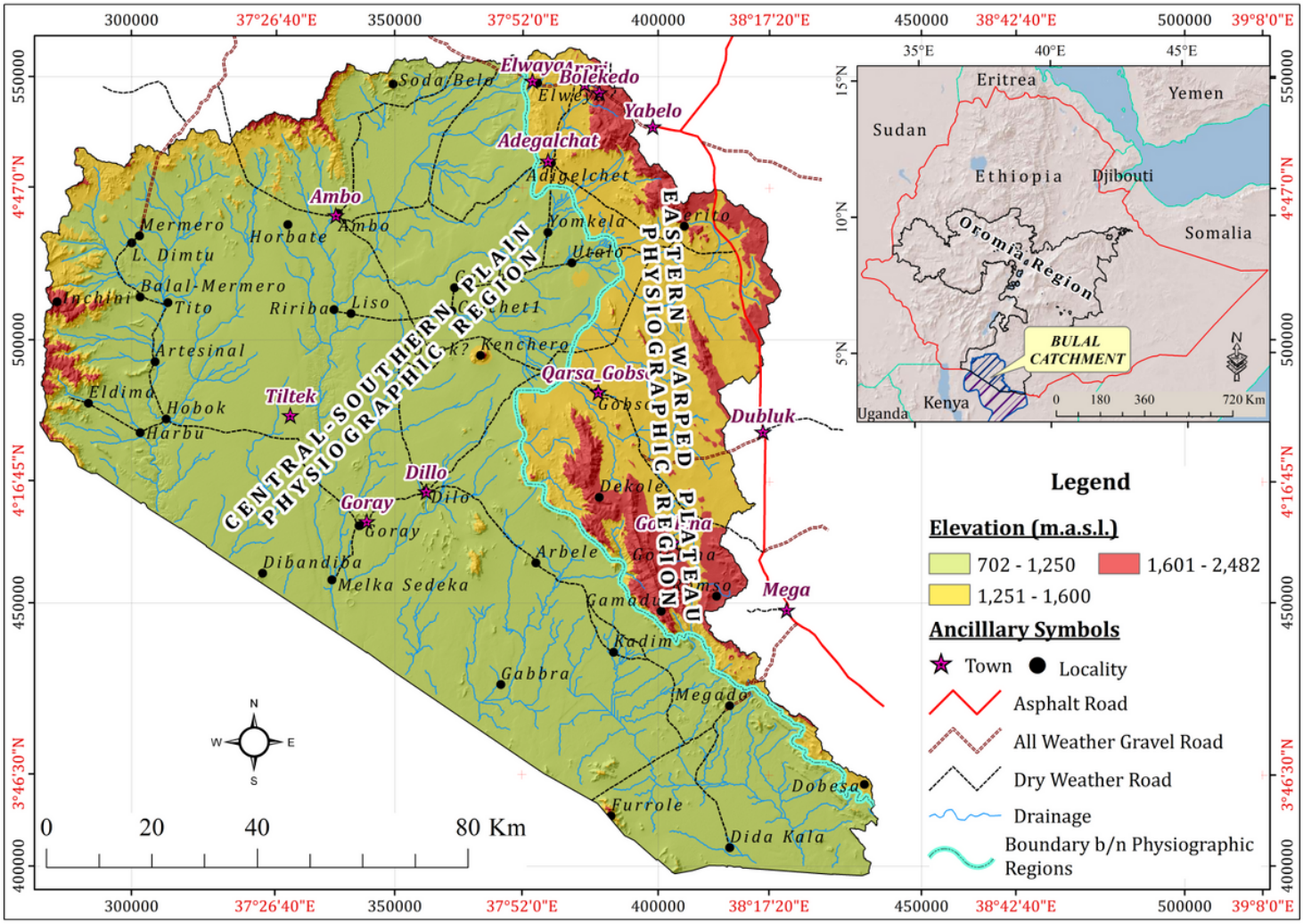

Figure 1

Location and physiographic map of the Bulal catchment.

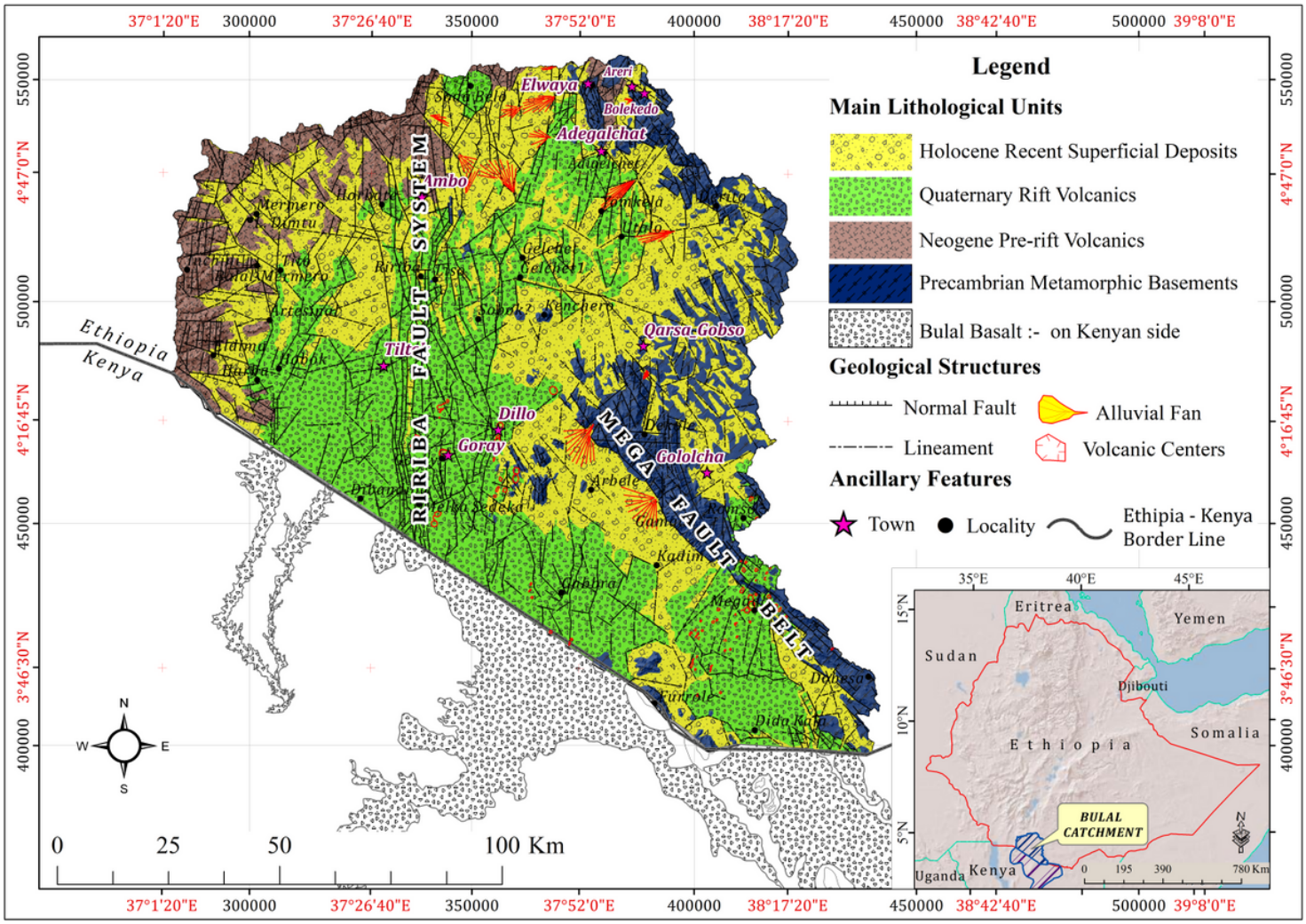

Figure 2

Geological map of the Bulal catchment (modified after Razak et al. 2020; Gebeyehu et al. 2022).

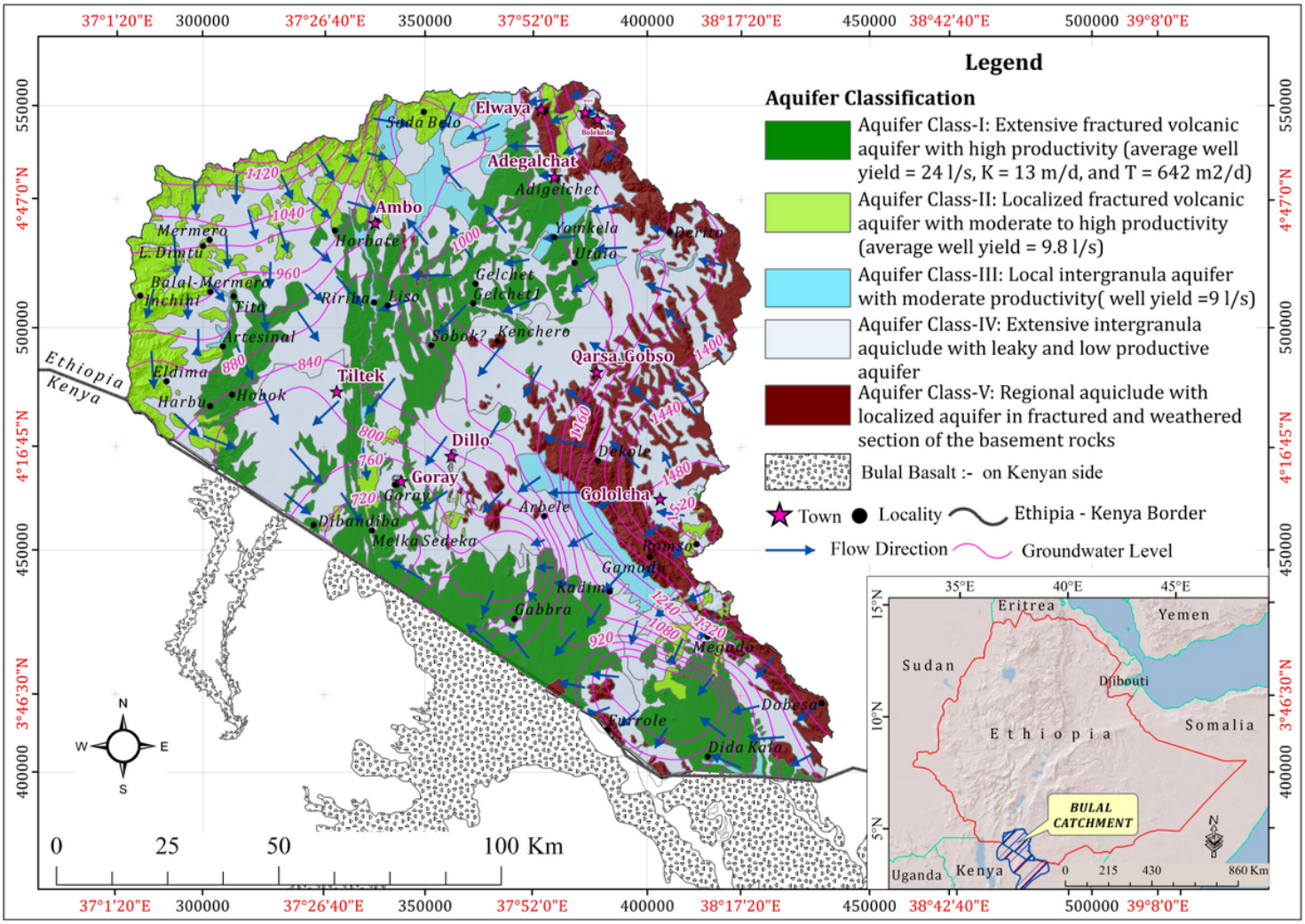

Figure 3

Hydrogeological map of the Bulal catchment (modified after OWWDSE 2017 and Gebeyehu et al. 2022).

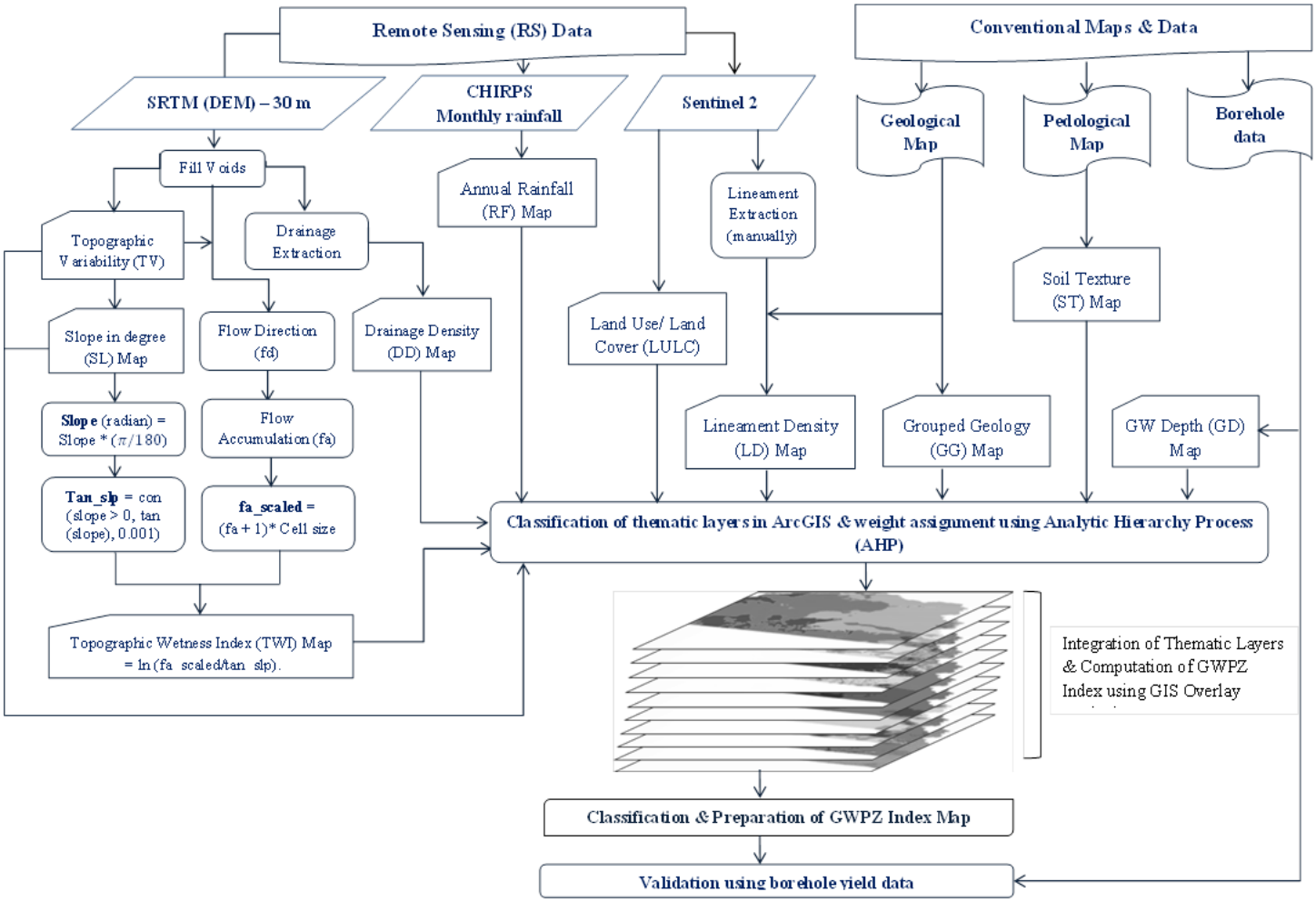

Figure 4

Flowchart of the methodology used for delineating groundwater potential zones.

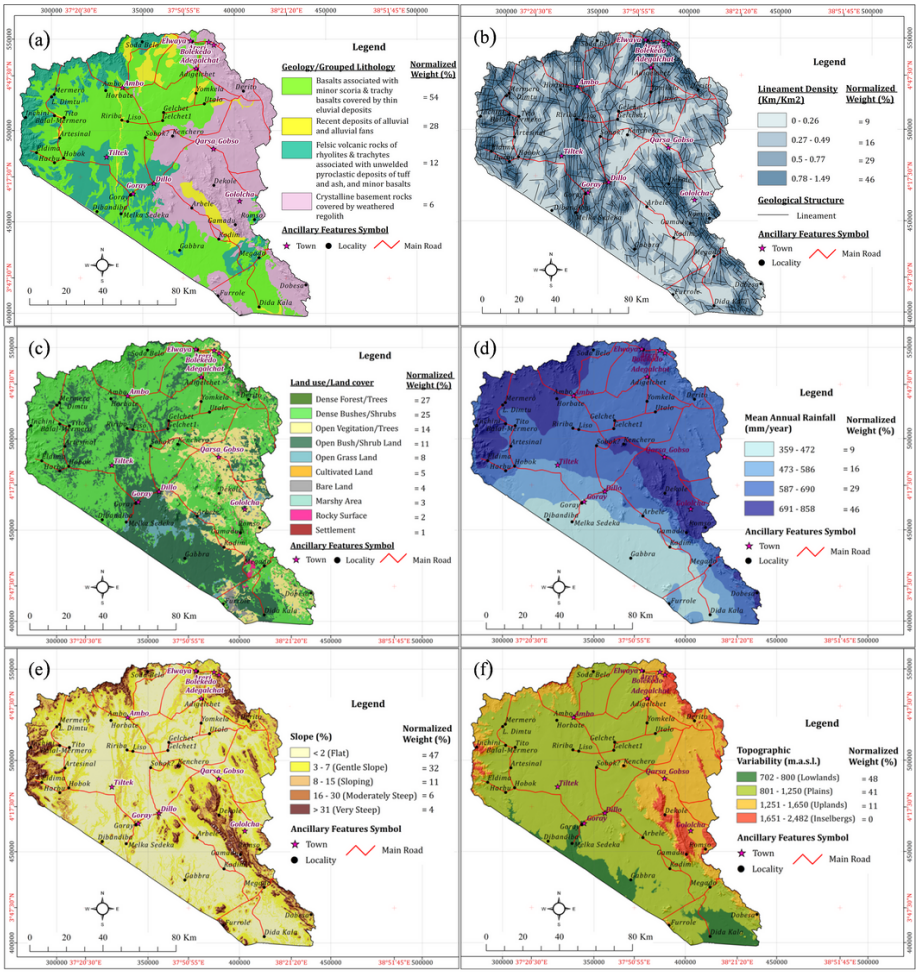

Figure 5

Weighted map layer of (a) grouped geology/lithology, (b) lineament density, (c) land used/land cover, (d) rainfall, (e) slope, and (f) topographic variability.

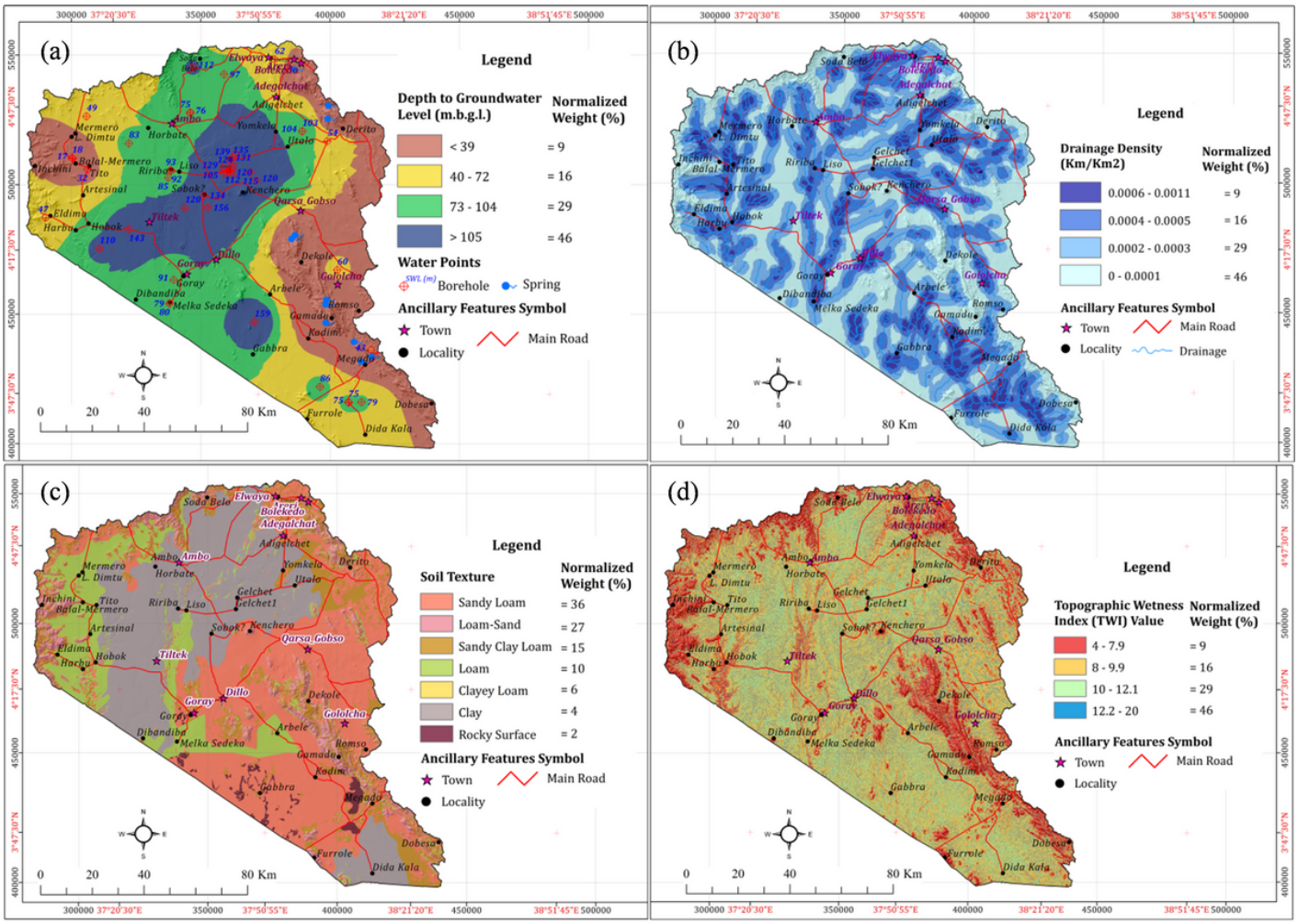

Figure 6

Weighted map layer of (a) depth to groundwater, (b) drainage density, (c) soil texture, and (d) topographic wetness index.

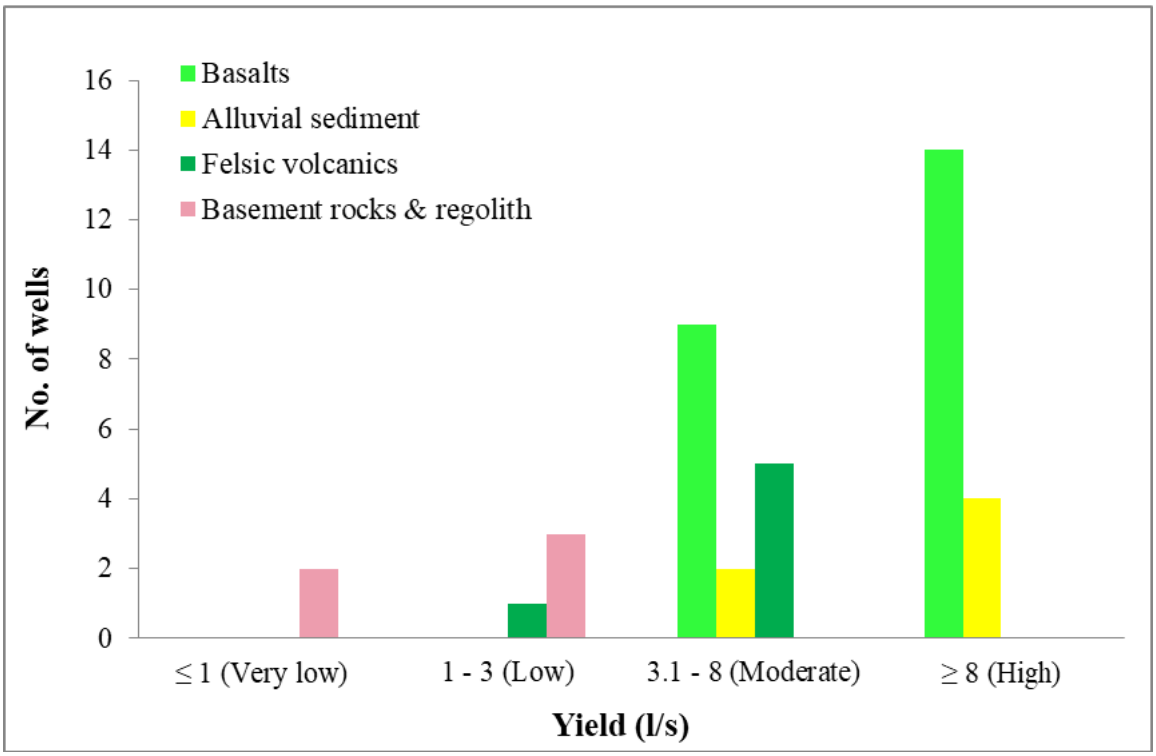

Figure 7

Groundwater potential zones index (GWPZI) map of the Bulal catchment.

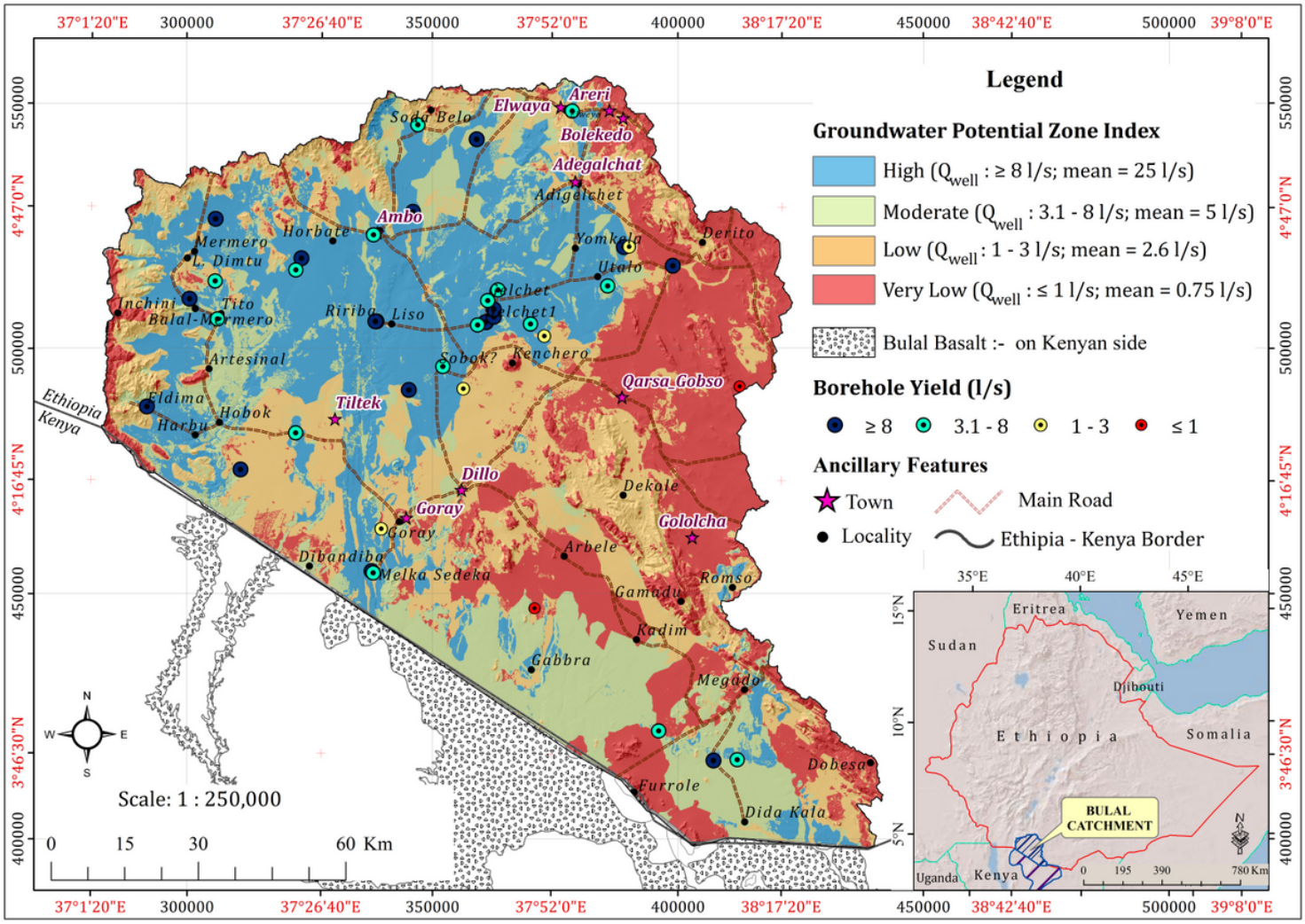

Figure 8

Well yields in different lithological units of the Bulal catchment.